Engine Dynamic Analysis With General Nonlinear Finite-Element Codes, Part 1: Overall Approach and Development of Bearing Damper Element

M. L. Adams
Associate Professor of Mechanical Engineering.

J. Padovan
Professor of Mechanical Engineering.

D. G. Fertis
Professor of Civil Engineering.

University of Akron, Akron, Ohio 44325

There is currently a considerable interest and level of activity in developing computational schemes to predict general engine dynamic behavior. The general feeling among researchers working on engine vibration problems is that various modes of operation, such as blade-loss events, require a high level of analysis sophistication to realistically model the engine. Proper account of system nonlinearities (particularly at the bearings, dampers and rubs) appears to be necessary if analytical predictions are to be realistic. The approach described in this paper seeks to make use of already proven general finite-element nonlinear time-transient computer codes which are available on the open market. The work specifically described in this paper covers the first phase of a three-phase NASA-Lewis-sponsored research grant on engine dynamic simulation with available finite element codes. The first phase was concentrated on the development of a bearing-damper element computer software package suitable for "plug-in" to available finite element codes.

Introduction and Background

Present-day jet engine configurations have evolved to a substantial degree through a trial-and-error process involving extensive testing. There are many fundamental dynamic phenomena which take place within these engines for which basic description and understanding have yet to be generated. Nonetheless, they work well. Modern aircraft engines are typical of current high-technology products in which the recently acquired computing capabilities of today are being used to better understand and improve what is already designed, built and operating.

A better understanding of the basic dynamic characteristics of existing and new engine configurations is a prerequisite for producing acceptable engine efficiencies on advanced configurations (i.e., smaller rotor/stator running clearances). Also, a better definition of engine dynamic response would more than likely provide valuable information and insights leading to reduced maintenance and overhaul costs on existing configurations. Furthermore, application of advanced engine dynamic simulation methods could potentially provide a considerable cost reduction in the development of new engine configurations by eliminating some of the trial-and-error process done with engine hardware development.

The emergence of advanced finite element codes, such as NASTRAN, NONSAP, MARC, ADINA, ANSYS and ABAQUS and related algorithmic advances, have placed comprehensive engine system dynamic analyses within reasonable reach. What remains to be done is to develop new component element software to properly model engine rotor/stator interactive components, such as the squeeze-film damper, within the algorithmic logic of already proven finite element codes. This is the major mission of this work.

For good reasons, aircraft gas turbine engines use rolling element bearings exclusively. This design philosophy has, until recent years, deprived engines of the beneficial damping inherent in many other types of rotating machinery where fluid-film journal bearings are used. The implementation of squeeze-film dampers in recent engine designs has now provided engine designers with an effective means of vibration energy dissipation. The net result is that engines with squeeze-film dampers are less sensitive to residual rotor imbalance and better able to control vibration and transmitted force levels resulting from various excitation sources within the engine.

The field of rotor dynamics has evolved to its present state primarily through the solution to problems in classes of machinery older than aircraft engines. In most other types of rotating machinery (e.g., steam turbines, centrifugal pumps and compressors, fans, generators, motors, etc.) the rotor can

Contributed by the Gas Turbine Division and presented at the International Gas Turbine Conference and Products Show, Houston, Texas, March 9–12, 1981 of THE AMERICAN SOCIETY OF MECHANICAL ENGINEERS. Manuscript received at ASME Headquarters December 15, 1980. Paper No. 81-GT-151.

be adequately modeled as an Euler or Timoshenko beam [1]. In addition, the support structure holding each bearing can often be adequately modeled as a separate mass-damping-stiffness path to ground (i.e., to the inertial frame). Also, for most purposes, bearing dynamic properties are characterized as stiffness and damping elements, linearized for small vibration amplitudes about some static equilibrium state. With few exceptions (e.g., Hibner [2]), it is this level of sophistication that has been utilized for the most part is rotor-dynamics analyses of aircraft engines.

Present day aircraft engines are structurally far more complex than most other types of rotating machinery. The multi-shaft configuration, plus the fact that the shafts are thin rotating shells, creates unique but significant complicating differences between aircraft engines and other machinery. Also, the stator structural support at each rotor bearing represents anything but a separate mass-damper-stiffness path to an inertial frame. In fact, setting the inertial frame for the engine is not a simple matter when the full range of in-service maneuvers is realized. Dynamic paths between different bearings exist not only through the rotor but through several other paths within the nonrotating engine structure, i.e., a "multi-level," multi-branch" system. As many as eight significant "levels" have been identified.

The feasibility of nonlinear dynamic analyses of multi-bearing flexible rotors has been recently demonstrated on non-aircraft applications [3]. There are highly nonlinear dynamic effects in aircraft engines, particularly under large excitation forces, such as blade or disk failures, hard landings, and foreign matter ingestion events.

Clearly, the field of aircraft engine dynamics is presently in a position where there is both a need for substantial advances and feasible means available by which such advances can be accomplished.

Time-Transient Nonlinear Dynamic Analyses

In recent years it has become evident that an important class of engine dynamic phenomena can not be studied without accounting for the highly nonlinear forces produced at bearings/dampers, labyrinths and other close-running rotor/stator clearances under large amplitude vibrations. In such cases, linear theory typically predicts vibration amplitudes larger than the actual running clearances. Furthermore, important vibratory phenomena, such as subharmonic resonance and motion limit cycles, are "filtered" out of the problem with a linear model, giving grossly erroneous predictions, qualitatively as well as quantitatively [3].

With few exceptions, nonlinear dynamics problems must be solved numerically as time-transient responses, whether the sought answer is a steady-state periodic motion or is strictly a transient phenomenon. The problem, is mathematically categorized as an initial value problem in which the displacements and velocities of the complete system must all be specified at the beginning of the transient. From that point forward in time, the equations of motion are numerically integrated (known as "marching") as far in time as one wishes to study the system motions and forces. If the system is dynamically stable, the transient motion dies out yielding the steady state response which in a system with a periodic force excitation will be a periodic motion. In a stable system with no time-varying force excitation, the transient will die out as the system comes to rest at one of its stable static equilibrium positions. If the system is unstable, the transient does not die out but continues to grow in time unless or until some nonlinear mechanism in the system limits the motion to what is frequently called a "limit cycle" [3].

In order to study the general dynamical characteristics of aircraft engines, nonlinear dynamics computational schemes

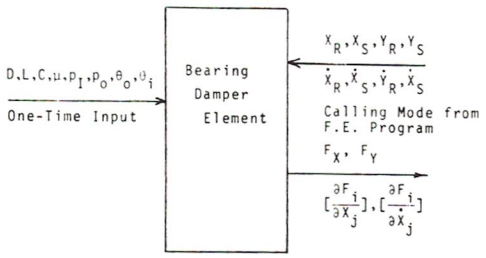

Fig. 1 Input/output of damper pilot code

are required. The approach taken is to develop software packages to model engine components which are not typically found on dynamical structures and therefore are not already built into existing nonlinear finite element structural dynamics computer codes. The initial effort has concentrated on developing such a software package for squeeze-film bearing dampers.

Overall Approach-Interactive Elements

Considering the typical engine structural complexities, an improved computational approach is necessary if a proper transient/steady-state model is to be developed for gas turbine engines. In this approach, it appears that the finite element method is one of the attractive modeling techniques for such problems. Its inherent capabilities include features essential to modern engines: 1) automatically handles multi-branch, multi-level structures in a more direct and efficient manner than flexibilities approaches, 2) well-suited to handle nonlinearities associated with structural kinematic and kinetic effects [4], 3) easily accommodates various types of boundary and constraint conditions, and 4) easily accommodates material nonisotropy and nonlinearity [4,5]. A body of established and proven algorithms are available which can handle these various important effects [4,6] as well as geometric complexities (e.g., beam, plate, 2-D and 3-D elements [7].

The required features which are presently not available with general purpose finite-element codes are provisions to handle rotor/stator interactive forces originating from squeeze-film dampers, seals and rub/impact events. Presented herein are the results of an effort to develop a squeeze-film damper computer software package which can be "plugged" into existing finite element codes. This work is detailed in the following section of this paper.

Squeeze-Film Damper Element

The bearing damper element is essentially an interactive element to represent squeeze film dampers. Its purpose is to bridge the "gap" between structural elements which are separated in the actual engine by a squeeze film damper. In its simplest version, it has an input/output setup as shown in Fig. 1. A source listing of this code is given in reference [8].

The rotor/stator interactive force generated in a bearing squeeze film damper is modeled using an adaptation of the classical Reynolds lubrication equation for incompressible laminar isoviscous films.

$$\frac{\partial}{\partial x}\left(\frac{h^3}{\mu}\frac{\partial p}{\partial x}\right)+\frac{\partial}{\partial z}\left(\frac{h^3}{\mu}\frac{\partial p}{\partial z}\right)=6\frac{\partial}{\partial x}(hU)+12\frac{dh}{dt} \qquad (1)$$

where

z = axial coordinate
x = circumferential coordinate = $r\theta$
h = local film thickness
$\frac{dh}{dt}$ = instantaneous local rate of change in h

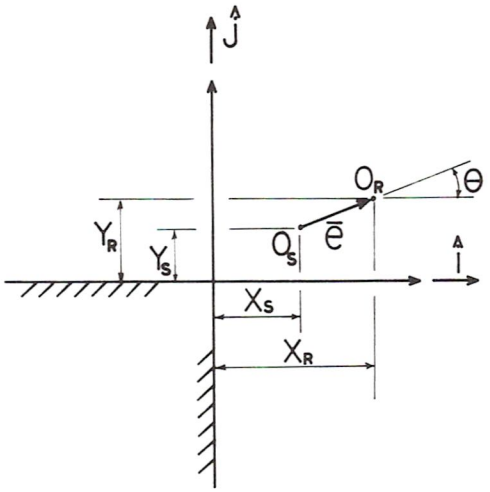

Fig. 2 Inertial coordinates

U = sliding velocity = $R\omega$, typically zero in a damper
C = radial clearance of damper annulus.

The relationship between system inertial coordinates and damper parameters comes through the expression for h, $\partial h/\partial x$ and dh/dt. Referring to Fig. 2, these relationships are summarized as follows:

$$\bar{e} = (X_R - X_S)\hat{i} + (Y_R - Y_S)\hat{j} \tag{2}$$

$$\dot{\bar{e}} = (\dot{X}_R - \dot{X}_S)\hat{i} + (\dot{Y}_R - \dot{Y}_S)\hat{j} \tag{3}$$

then

$$h = C - \bar{e}\cdot\hat{n} = C - (X_R - X_S)\cos\theta - (Y_R - Y_S)\sin\theta \tag{4}$$

$$\frac{\partial h}{\partial x} = \frac{1}{R}\frac{\partial h}{\partial \theta} = \frac{1}{R}[(X_R - X_S]\sin\theta - (Y_R - Y_S)\cos\theta] \tag{5}$$

and

$$\frac{dh}{dt} = -(\dot{X}_R - \dot{X}_S)\cos\theta - (\dot{Y}_R - \dot{Y}_S)\sin\theta \tag{6}$$

Typical configurations of dampers which are currently being employed in engines have done away with centering springs common in older designs. Design simplicity as well as centering-spring fatigue life are apparently the major reasons. Also, in the majority of cases, damper end seals are used because this keeps damper throughflow sufficiently low to be compatible with the overall engine lub system of pre-damper configurations. However, the disadvantage of having end seals is that a "large" damper clearance of typically 10 mils is required in order for the squeeze-film action to effectively dissipate vibration energy. From other considerations, a smaller damper clearance would be desireable (e.g., blade tip clearances). Without end seals, the optimum damper clearance is considerably smaller. Engines with higher oil flow capacity and no damper end seals are probably the trend on future designs.

Two typical configurations are shown in Figs. 3 and 4. The end seal configuration in Figs. 3 and 4(*a*) essentially divides the lubricant annulus into two pressure domains whereas that in Fig. 4(*b*) is a one-domain problem. In both cases, the "long-bearing" solution is appropriate. Conversely, without end seals a "short-bearing" type of solution is appropriate. Both solutions are options in the software package developed in this work.

For the "long-bearing" solution, $\partial p/\partial z << \partial p/\partial x$, and the following ordinary differential equation (two-point boundary value problem) is obtained from equation (1), (for $U = 0$).

$$\frac{d}{dx}\left(\frac{h^3}{\mu}\frac{dp}{dx}\right) = 12\frac{dh}{dt} \tag{7}$$

For configurations with no end seals, an improved adaptation of the short-bearing approach is used by implementing the parabolic assumption of O'Donoghue [9]. The following approximation is made.

$$p(\theta,z) = p(\theta,0)\left(1 - \frac{4z^2}{L^2}\right) \tag{8}$$

This assumes an axially symmetric axial pressure distribution at every circumferential location, and results in the following pressure field equation.

$$\frac{1}{\mu}\frac{\partial}{\partial x}\left(h^3\frac{\partial p}{\partial x}\right) = 12\frac{dh}{dt} + 8\frac{p(\theta,0)h^3}{L^2} \tag{9}$$

This is actually a first-order Fourier approximation using the parabola as the single approximative function.

A convergent approximation to the full two-dimensional Reynolds equation can be obtained, as an extension of the foregoing approach by O'Donoghue [9]. The number of Fourier terms is increased to N, resulting in N simultaneous ordinary differential equations.

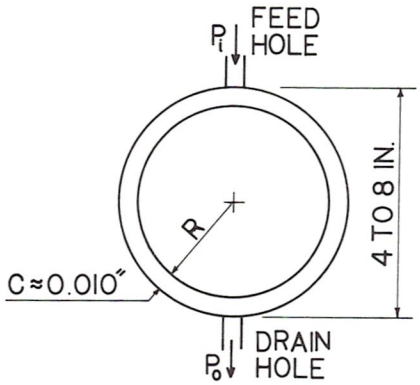

Fig. 3 A typical aircraft engine damper configuration

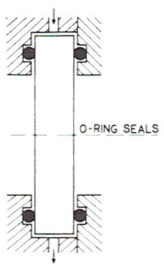

Fig. 4(*a*) Configuration frequently used in military applications

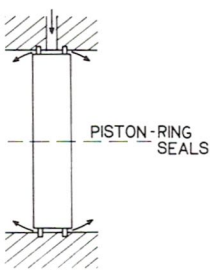

Fig. 4(*b*) Configuration frequently used in commercial applications

$$p(\theta,z) = p_1(\theta,0)\cos\frac{\pi z}{L} + p_2(\theta,0)\cos\frac{3\pi z}{L} + \ldots$$

$$+ p_N(\theta,0)\cos\frac{(2N-1)\pi z}{L} \tag{10}$$

Substitution into the general 2-D Reynolds equation (1), followed by LHS:RHS segregation by arguments yields N ordinary differential equations, one for each $p_i(\theta,0)$, [9].

Method of Solution

Although there are computationally fast closed-form solutions available such as given in [10,11], they do not retain sufficient generality to handle the specified pressure boundaries at supply and drain ports (Figs. 3,4,5) of typical configurations. Also, they are not amenable to structural deflections of the damper elements. For these reasons, the following approach has been used. Although somewhat computationally slower than closed-form solutions, it is nonetheless computationally quite efficient, and retains the generality deemed necessary. The solution method given below is used for all three formulations (i.e., equations (7) through (10). It is described below as implemented for the long-bearing formulation.

Based on a 3-point central difference, the following long-bearing equation yields equation (11).

$$h^3\frac{d^2p}{dx^2} + 3h^2\frac{dh}{dx}\frac{dp}{dx} = 12\mu\frac{dh}{dt}$$

$$\left(\frac{dp}{dx}\right)_i \cong \frac{P_{i+1}-P_{i-1}}{2\Delta x}$$

$$\left(\frac{d^2p}{dx^2}\right)_i \cong \frac{P_{i+1}-2P_i+P_{i-1}}{\Delta x^2}$$

$$h_i^3\left(\frac{P_{i+1}-2P_i+P_{i-1}}{\Delta x^2}\right) + 3h_i^2\frac{dh_i}{dx}\left(\frac{P_{i+1}-P_{i-1}}{2\Delta x}\right) =$$

$$12\mu\frac{dh_i}{dt} \tag{11}$$

Rearranging (11) produces

$$\underbrace{P_{i+1}\left[\frac{h_i^3}{\Delta x^2} + \frac{3h_i^2}{2\Delta x}\frac{dh_i}{dx}\right]}_{D_j} + \underbrace{P_i\left[-\frac{2h_i^3}{\Delta x^2}\right]}_{C_j} +$$

$$\underbrace{P_{i-1}\left[\frac{h_i^3}{\Delta x^2} - \frac{3h_i^2}{2\Delta x}\frac{dh_i}{dx}\right]}_{E_j} = \underbrace{12\mu\frac{dh_i}{dt}}_{R_j}$$

which is condensed to the following form.

$$C_jP_j + E_jP_{j-1} + D_jP_{j+1} = R_j \tag{12}$$

Employing the recursion relationship,

$$P_{j-1} = A_jP_j + B_j \tag{13}$$

equation (12) can be expressed in terms of only two adjacent grid points as follows

$$C_jP_j + E_j(A_jP_j + B_j) + D_jP_{j+1} = R_j \tag{14}$$

or

$$P_j(C_j + E_jA_j) + E_jB_j + D_jP_{j+1} = R_j \tag{15}$$

Therefore,

$$P_j = \left(\frac{-D_j}{C_j + E_jA_j}\right)P_{j+1} + \frac{R_j - E_jB_j}{C_j + E_jA_j} \tag{16}$$

which when compared to equation (13), yields the following recursion relationships:

$$A_{j+1} = -\frac{D_j}{C_j + E_jA_j} \tag{17}$$

$$B_{j+1} = \frac{R_j - E_jB_j}{C_j + E_jA_j} \tag{18}$$

From the upstream boundary condition for each domain, the $\{A\}$ and $\{B\}$ vectors are determined by starting with $A_2 = 0$, $B_2 = P_1$ (called the forward sweep).

The downstream boundary condition is inserted at the beginning of the backward sweep as follows.

$$\begin{aligned} P_{M-1} &= A_MP_M + B_M \\ P_{M-2} &= A_{M-1}P_{M-1} + B_{M-1} \\ &\vdots \quad\quad \vdots \\ P_2 &= A_3P_3 + B_3 \end{aligned} \tag{19}$$

Film rupture is handled by the following substitution. If $P_j < P_{\text{vapor}}$, set $P_j = P_{\text{vapor}}$ before computing P_{j-1}. This is equivalent to the condition $\partial p/\partial x = 0$ at the film-rupture, full-film boundary. In the case of the 2-D convergent approach indicated by equation (10), this point-by-point test is made on the local summation.

$$P(\theta_j,z) = \sum_{k=1}^{N} P_k(\theta_j,z).$$

The method of solution, although not closed-form, is noniterative and is a 1-D adaptation of the 2-D finite difference method of Castelli and Shapiro [12]. While it does entail a one-dimensional, finite-difference scheme, it requires only a very small amount of CPU time and is therefore ideally suited to time transient rotor dynamics analyses. It has major advantages over the purely closed-form approximations, e.g., [10,11], as noted earlier. These major advantages are immediate account of specified-pressure boundary conditions at feed and drain holes of a damper. Also, the finite difference approach easily permits account of static as well as dynamic deflections which alter the oil film gap geometry from ideal rigid circular shapes.

Force and Force Gradients. Forces components on rotor are computed by numerical integration of the instantaneous film pressure distribution, as is standard.

$$\begin{aligned} F_X &= -\int_{A^p}\cos\theta dA = -LR\int_{\theta_1}^{\theta_2} p(\theta)\cos\theta d\theta \\ F_Y &= -\int_{A^p}\sin\theta dA = -LR\int_{\theta_1}^{\theta_2} p(\theta)\sin\theta d\theta \end{aligned} \tag{20}$$

Stator force components are equal but opposite the rotor force components.

Force gradients (i.e., instantaneous tangent stiffness and damping) components are obtained by local "small" perturbations, as is standard.

$$[C_{ij}]_{2\times 2} = \left[-\frac{\partial F_j}{\partial \dot{X}_j}\right]; \quad [K_{ij}]_{2\times 2} = \left[-\frac{\partial F_i}{\partial x_j}\right] \tag{21}$$

where

$$\frac{\partial F_i}{\partial \dot{X}_j} \simeq \frac{\Delta F_i}{\Delta \dot{X}_j}; \quad \frac{\partial F_i}{\partial X_j} \simeq \frac{\Delta F_i}{\Delta X_j} \tag{22}$$

Numerical differentiation is performed with small $\Delta\dot{X}_j$ and ΔX_j increments about instantaneous conditions. This provides continuous updating of $\{F_j\}$, $[C_{ij}]$ and $[K_{ij}]$.

Application of Damper Element

For purposes of checking out the damper element coded and to demonstrate its use, two types of computations were made. First, a parametric study of damper pressure

distributions was made for a variety of specified circular orbits, for both long-bearing and short-bearing solutions. Second, a four-degree-of-freedom rotor-damper-stator model was investigated under conditions of small rotor unbalance through large rotor unbalance. These results are summarized below.

For the parametric study on pressure distribution, the following damper annulus parameters were used:

Diameter, $D = 6$ in.
Length, $L = 1.25$ in.
Radial clearance, $C = 0.010$ in.
Lubricant viscosity, $\mu = 1 \times 10^{-6}$ reyns
Angle between inlet oil port and drain port, $(\theta_i - \theta_0) = 180$ deg
Inlet oil port pressure, $P_i = 55$ psia
Drain port pressure, $p_0 = 15$ psia

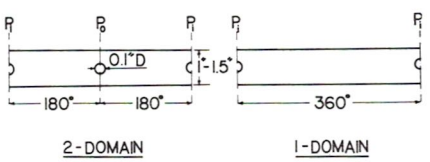

Fig. 5 Unwrapped squeeze-film pressure solution domains for configurations shown in Fig. 4

Lubricant vapor pressure, $p_v = 1.5$ psia
Orbit angular velocity, $\Omega = 3600$ cpm (377. rad/sec)

The above damper parameters are typical for modern gas turbine aircraft engines. A parametric study was made postulating the outer ring of the damper fixed and the inner ring having a constant-radius constant-velocity concentric orbit. Eccentricity ratios (i.e., orbit radius/radial clearance) from 0.05 to 0.95 were computed, both for the long-bearing and short-bearing solutions.

Circumferential center-line pressures were plotted as a function of circumferential position and time, for one period of prescribed motion. The results for the long-bearing solution are shown in Fig. 6, and for the short-bearing solution in Fig. 7. The difference between long-bearing and short-bearing solution is quite large when compared with the same radial clearance. One therefore sees why dampers with no end seals require smaller clearances to work properly than dampers with end seals.

A simple "driver" code was written (see listing [8]) which uses the damper-element code in the same manner as a general application with large finite element codes. The "driver" code is based on a four-degree-of-freedom system, i.e., planar motion of the inner and outer damper elements. This then simulates a single-mass rotor connected to a single-mass stator via the damper element. The system analyzed is shown in Fig. 8. The model is coded to simulate arbitrary rotating

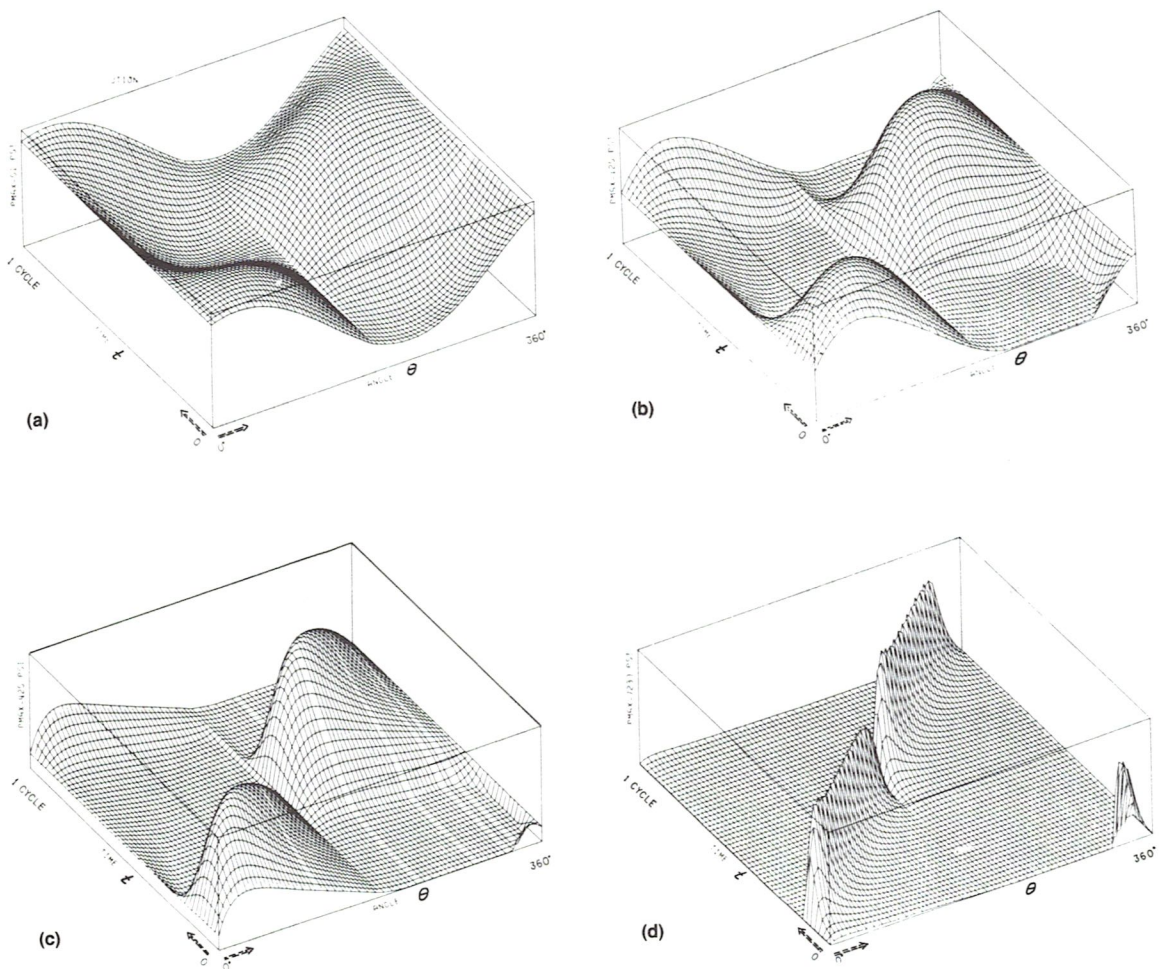

Fig. 6 Pressure distribution in circumferential direction and time of one cycle of circular orbit (long-bearing solution) (*a*) $e/c = 0.05$, (*b*) $e/c = 0.20$, (c) $e/c = 0.60$, (*d*) $e/c = 0.95$

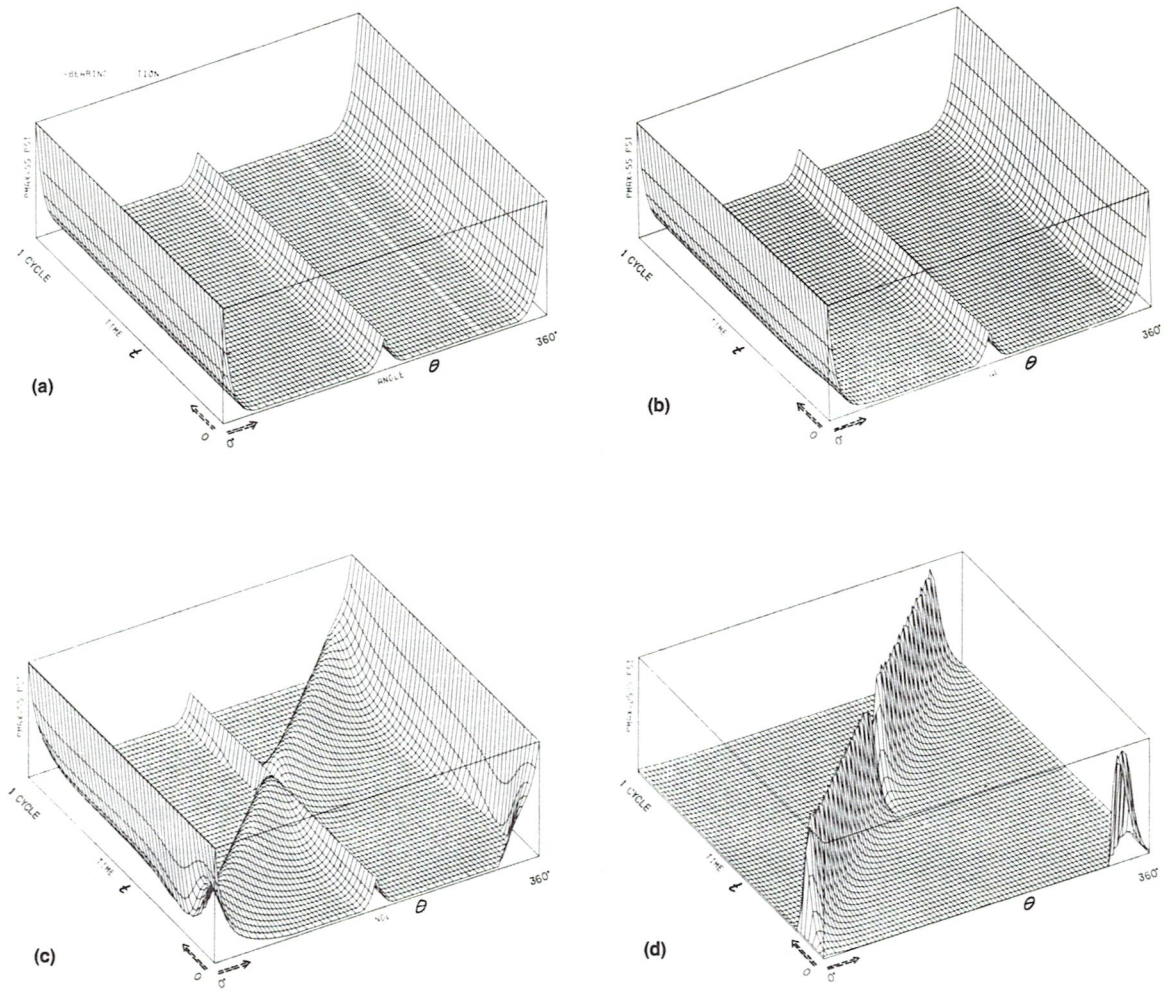

Fig. 7 Pressure distribution in circumferential direction and time of one cycle of circular orbit (short-bearing solution), (*a*) $e/c = 0.05$, (*b*) $e/c = 0.20$, (*c*) $e/c = 0.6$, (*d*) $e/c = 0.95$

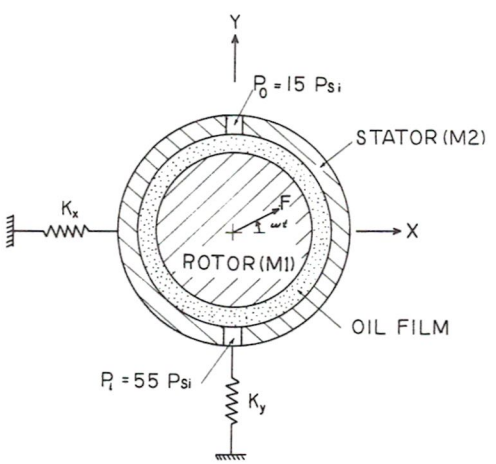

Fig. 8 Simple 2-mass, 4-degree-of-freedom test case (same damper parameters as on page 5)

and/or static radial loads. Aside from demonstration purposes, this four-degree-of-freedom model has been devised to check against the same type of system when executed with the damper element implanted into the general purpose nonlinear finite element code ADINA.

Note from Fig. 8 that the high-pressure port (i.e., feed port) is located on the bottom of the damper so as to assist "lift-off". Since centering springs are not typically used, they have been excluded in this example. Lift-off therefore requires some amount of vibration to overcome the dead-weight load. Rotating unbalance loads of 100, 200, 300, 500, and 1000 lbs were run with $\Omega = 150$ rad/s. Orbital plots were made showing rotor and stator total motion on one plot and rotor-relative-to-stator motion on a second plot. The plotted results are shown in Figs. 9 through 13.

For a 100 lb rotating load (Fig. 9) the motions shown are for a 20 cycle transient from time = 0. The rotor and stator each show close to the same motion, and their relative motion is small, with the rotor barely "lifting off". The relative orbit is essentially oscillatory. However, when the rotating load is increased to 200 lbs, (Fig. 10), the relative orbital motion shows the beginnings of orbital motion, i.e., a "cresent moon" shape as measured by numerous investigators. Further increase in magnitude of the rotating load to 300 lbs (Fig. 11) shows a well-defined steady-state total motion as well as relative motion. Note that with a 300 lbs rotating load, the relative (rotor-to-stator) orbit is still small in comparison to the radial damper clearance and confined to the region of the bottom of the damper. However, an increase of rotating load magnitude to 500 lbs causes a considerable change to the relative orbit (Fig. 12). Notice now that the relative motion of the rotor with respect to the stator fills a major portion of the

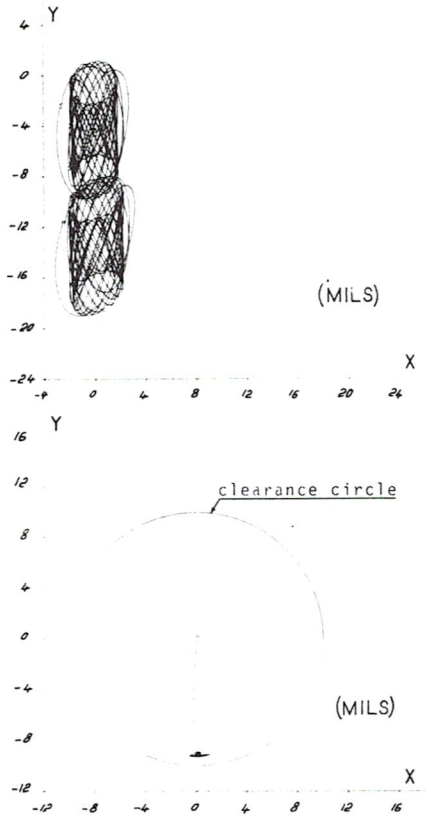

Fig. 9 Nonlinear dynamic transient of simple 4 DOE system (see Fig. 8) $|F|$ = 100 lbs, ω = 150 rad/s, M1 = M2 = 500 lbs, $Kx = Ky = 116{,}000$ lbs/in.

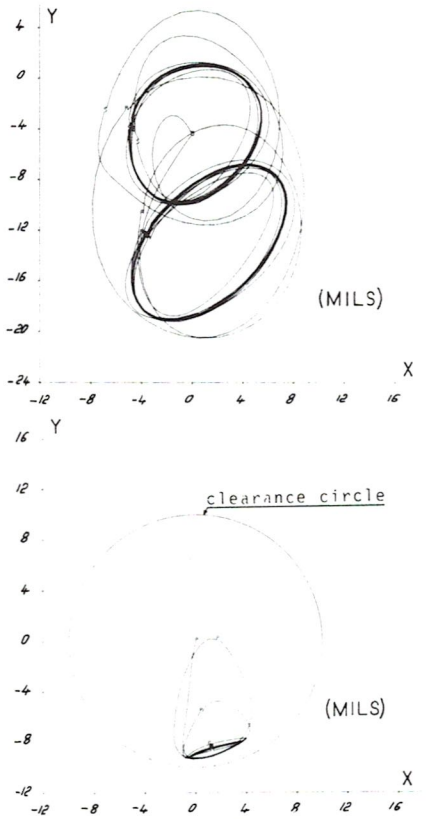

Fig. 11 Nonlinear dynamic transient of simple 4 DOE system (see Fig. 8) $|F|$ = 300 lbs, ω = 150 rad/sec, M1 = M2 = 500 lbs, $Kx = Ky = 116{,}000$ lbs/in.

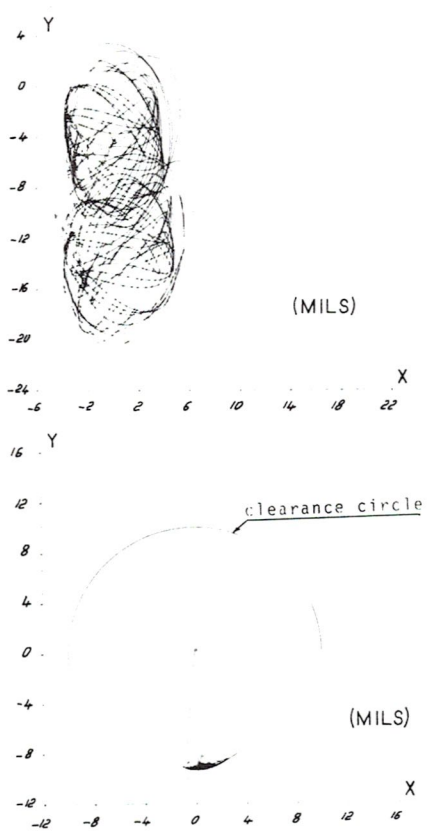

Fig. 10 Nonlinear dynamic transient of simple 4 DOE system (see Fig. 8) $|F|$ = 200 lbs, ω = 150 rad/s, M1 = M2 = 500 lbs, $Kx = Ky = 116{,}000$ lbs/in

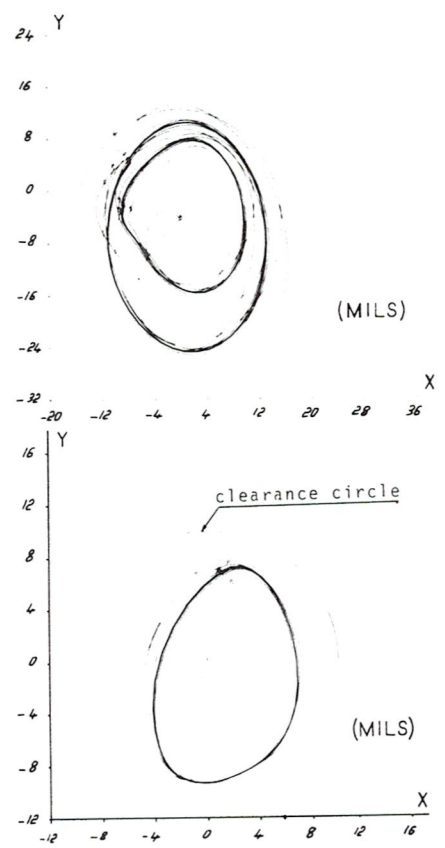

Fig. 12 Nonlinear dynamic transient of simple 4 DOE system (see Fig. 8) $|F|$ = 500 lbs, ω = 150 rad/s, M1 = M2 = 500 lbs, $Kx = Ky = 116{,}000$ lbs/in.

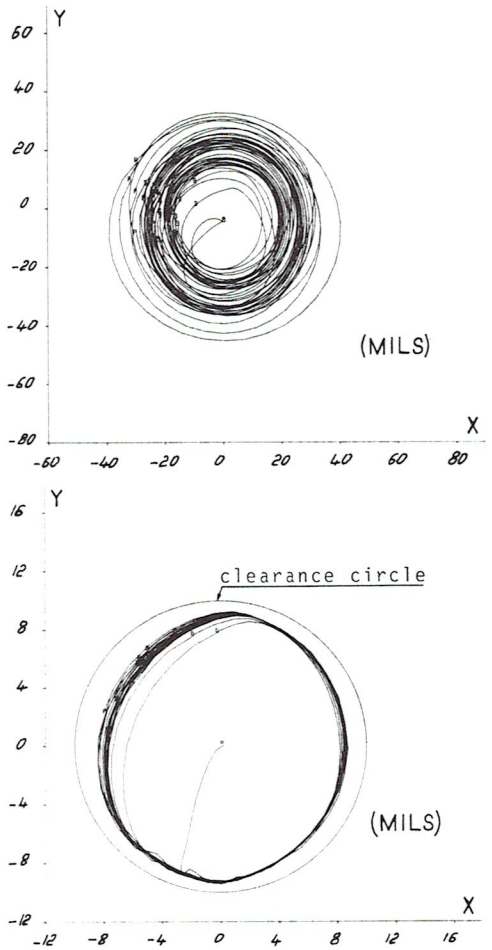

Fig. 13 Nonlinear dynamic transient of simple 4 DOE system (see Fig. 8) $|F|$ = 1000 lbs, ω = 150 rad/s, M1 = M2 = 500 lbs, $Kx = Ky = 116{,}000$ lbs/in.

clearance circle. Further increase of rotating load magnitude to 1000 lbs (Fig. 13) simply causes the steady-state relative orbit to expand and fill even more of the damper clearance circle.

Summary

This paper summarizes the work completed on the first-year effort of a three-year project. A detailed scope of work for the remaining two-year effort is given in reference [8]. The work completed and presented in this paper has produced (*i*) an overall solution strategy to the general engine dynamics problem, (*ii*) a clear definition of where present efforts should be concentrated to utilize available and proven FE codes, and (*iii*) a squeeze-film damper software package ready for implant into available FE codes.

Acknowledgment

The work reported in this paper was sponsored by NASA Lewis Research Center under NASA Grant NSG-3283. The NASA coordinator on this grant was Dr. C. C. Chamis, whose suggestions and encouragement are greatly appreciated.

References

1 Fertis, D. G., "Dynamics and Vibrations of Structures," Wiley, New York, 1973.

2 Hibner, D. H., "Dynamic Response of Viscous-Damped Multi-Shaft Jet Engines," *AIAA Journal of Aircraft,* Vol. 12, 1975, pp. 305–312.

3 Adams, M. L., "Nonlinear Dynamics of Flexible Multi-Bearing Rotors," *Journal of Sound and Vibration,* Vol. 71, No. 1, 1980, pp. 129–144.

4 Belytschko, T., "Nonlinear Analyses-Descriptions and Numerical Stability," *Computer Programs in Shock and Vibration,* ed., W. Pilkey and B. Pilkey, Shock and Vibration Information Center, Washington, D.C., 1975, pp. 537.

5 Zienkiewicz, O. D., "The Finite Element Method," McGraw Hill, London, 1977.

6 Felippa, C. A., and Park, K. C., "Direct Time Integration Methods in Nonlinear Structural Dynamics," presented at FENOMECH, University of Stuttgart, 1978.

7 *Structural Mechanics Computer Programs,* edited by Pilkey, W., Saczalski, K. and Schaeffer, H., University Press of Virginia, Charlottsville, 1975.

8 Adams, M. L., Padovan, J., and Fertis, D. G., "Finite Elements for Rotor/Stator Interactive Forces in General Engine Dynamic Simulation, Part 1: Development of Bearing Damper Element," (to appear as NASA Report on Grant NSG-3283).

9 O'Donoghue, J. P., Koch, P. R., and Hooke, C. J., "Approximate Short Bearing Analysis and Experimental Results Obtained Using Plastic Bearing Liners," *Proc. Institute of Mechanical Engineers,* Vol. 194, 1969, pp. 190–196.

10 Rhode, S. M., and Li, D. F., "A Generalized Short Bearing Theory," ASME *Journal of Lubrication Technology,* Vol. 102, No. 3, 1980, pp. 278–282.

11 Barrett, L. E., Allaire, P. E., and Gunter, E. J., "A Finite Length Bearing Correction Factor for Short Bearing Theory," ASME *Journal of Lubrication Technology,* Vol. 102, No. 3, 1980, pp. 283–290.

12 Castelli, V., and Shapiro, W., "Improved Method for Numerical Solutions of the General Incompressible Fluid Film Lubrication Problem," ASME *Journal of Lubrication Technology,* Vol. 89, No. 2, 1967, pp. 211–218.